Large-scale aligned silicon carbonitride nanotube arrays: Synthesis, characterization, and field emission property

L. LiaoZ. Xu, K. H. Liu, W. L. Wang, S. Liu, X. D. Bai, and E. G. WangJ. C. Li and C. Liu

Large-scale aligned silicon carbonitride nanotube arrays: Synthesis, characterization, and field emission property

L. Liao
Institute of Physics, Chinese Academy of Sciences, Beijing 100080, China and Department of Physics, Wuhan University, Wuhan 430072, China

Z. Xu, K. H. Liu, W. L. Wang, S. Liu, X. D. Bai, and E. G. Wang[a)]
Institute of Physics, Chinese Academy of Sciences, Beijing 100080, China

J. C. Li and C. Liu
Department of Physics, Wuhan University, Wuhan 430072, China

Large-scale aligned silicon carbonitride (SiCN) nanotube arrays have been synthesized by microwave-plasma-assisted chemical vapor deposition using SiH_4, CH_4, and N_2 as precursors. The three elements of Si, C, and N are chemically bonded with each other and the nanotube composition can be adjusted by varying the SiH_4 concentration, as revealed by electron energy loss spectroscopy and x-ray photoelectron spectroscopy. The evolution of microstructure of the SiCN nanotubes with different Si concentrations was characterized by high-resolution transmission electron microscopy and Raman spectroscopy. The dependence of field emission characteristics of the SiCN nanotubes on the composition has been investigated. With the increasing Si concentration, the SiCN nanotube exhibits more favorable oxidation resistance, which suggests that SiCN nanotube is a promising candidate as stable field emitter. © *2007 American Institute of Physics*. [DOI: 10.1063/1.2738378]

I. INTRODUCTION

Since a nanostructured field emitter has the advantage with respect to power efficiency and a reduction in device size compared to the conventional thermionic emitter, a variety of nanomaterials have been studied for the field emission use.[1–3] Among them, the field emission of carbon nanotubes (CNTs) has been most widely studied.[4–9] However, the field emission of CNTs undergoes unavoidable degradation under oxygen ambient,[10–12] which is one of the hurdles for their applications.[13] It is expected that the electron emitters have high oxidation resistance in order to increase the emitter lifetime.

Recently, silicon carbon nitride (SiCN) nanowires with large length (several tens of microns) and well crystal facets have been grown.[14,15] The ternary SiCN compound constitutes an important wide-band gap semiconducting material within the blue-ultraviolet spectral region[16,17] and has excellent mechanical properties with high hardness and bulk modulus.[18] SiCN could withstand high temperatures over 1500 °C without oxidation,[19] which shows great interest for their applications as the high oxidation-resistance semiconductor field emitters.

In this article, the tubular structure of SiCN has been achieved. Large-scale aligned SiCN nanotube arrays were synthesized by microwave-plasma-assisted chemical vapor deposition (MPCVD). The microstructures of the SiCN nanotubes were characterized systematically. The field emission properties of the SiCN nanotubes and their oxidation-resistance behaviors were investigated.

II. EXPERIMENTS

The samples were synthesized by MPCVD (ASTeX 2115) apparatus, which had been used to prepare nitrogen containing nanoscale diamond films[20] and carbon nitride nanotubes (CNNTs).[21,22] In this study, $SiO_2/Si(111)$ wafers were used as substrates. The iron films were deposited onto the substrates by sputtering. The catalyst-coated substrate is placed in a CVD stainless steel chamber with a base pressure of below 0.5 Pa. After pretreatment by N_2 plasma for 5 min, SiH_4, CH_4, and N_2 are introduced into the chamber with flow rates of 0–20, 120, and 20 sccm, respectively. The microwave power is 650 W. The temperature on the surface of graphite stage is maintained at 650 °C by a radio-frequency heat source and the reactive pressure is set at 2.8 kPa. The growth time is about 30 min.

The as-grown samples were characterized using Sirion FEG scanning electron microscope (SEM), JEOL JEM 2010 FEG high-resolution transmission electron microscope (HR-TEM) equipped with electron energy loss spectroscopy (EELS), ESCALAB-5 x-ray photoelectron spectroscopy (XPS), and JY-T64000 Raman microspectroscopy. The field electron emission properties were investigated with a home-made system.[23]

III. RESULTS AND DISCUSSION

A. Nanotube structure

Figure 1 is a SEM image of the as-grown large-scale SiCN nanotube arrays. It shows that the SiCN nanotubes are well aligned and uniformly distributed at a high density. The nanotubes are 6−7 μm in length and 100–200 nm in diameter.

---

a)Author to whom correspondence should be addressed; electronic mail: egwang@aphy.iphy.ac.cn
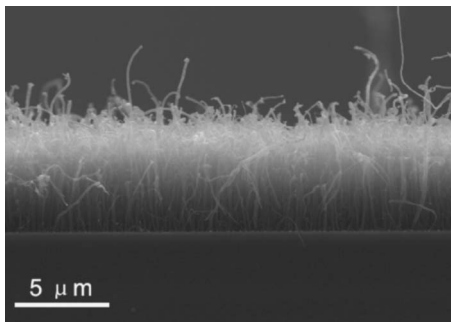
FIG. 1. A SEM image showing large-scale aligned SiCN nanotube arrays on Si substrates.

The typical TEM image indicates the SiCN nanotubes are multiwalled partially hollow structure, as shown in Fig. 2(a). Different from the pure carbon nanotubes, the SiCN nanotubes contain several transverse layers inside the inner-
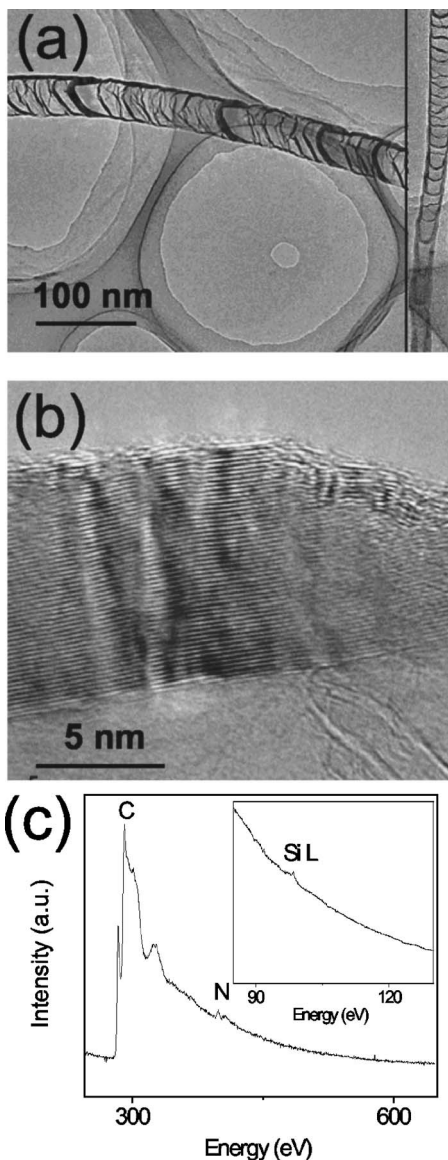

FIG. 2. (a) A typical TEM image of the SiCN nanotubes, its inset shows the CN/SiCN nanotube heterojunction prepared by two-stage growth, (b) high-resolution TEM image of the SiCN nanotube walls; and (c) EELS spectrum from a SiCN nanotube.

most wall, it is similar to the nitrogen-doped carbon nanotubes produced by microwave-plasma chemical vapor deposition.[22] The inset of Fig. 2(a) shows a heterojunction formed by CNNT and SiCN nanotube, in which the upside is the SiCN nanotube and the downside is the CNNT. The fabrication method is the same as that of CNT/CNNT heterojunctions.[24] Figure 2(b) is a HRTEM image indicating the walls of SiCN nanotube are well graphitized. The EELS spectrum of a single SiCN nanotube is given in Fig. 2(c). The K-shell ionizations of C and N are at 284 and 401 eV, respectively, and the L-shell ionization of Si is at 99 eV. The carbon and nitrogen regions show sharply defined π^* and σ^* edges, which are characteristic of sp^2 hybridization of the graphite-like structure. The feature of the nitrogen K edge is consistent with that of the covalent nitrogen in a hexagonal lattice,[25] revealing the chemically bonded N atoms in the SiCN nanotube.

B. XPS characterization

XPS is applied to further determine the sample chemical composition and the bond state among Si, C, and N in the SiCN nanotubes. The spatial resolution is less than 2 μm. Figure 3(a) is the broad XPS spectra for the three samples synthesized by different SiH$_4$ concentrations in precursor gas mixture. It is shown that the Si concentrations are in a large range from 0 to 11 at. %, they are $C_{0.92}N_{0.08}$ (0 sccm SiH$_4$), $Si_{0.05}C_{0.88}N_{0.07}$ (8 sccm SiH$_4$), and $Si_{0.11}C_{0.76}N_{0.13}$ (20 sccm SiH$_4$), respectively. Figures 3(b)–3(d) depict the high-resolution XPS scan of the C(1s), N(1s), and Si(2p) peaks of $Si_{0.11}C_{0.76}N_{0.13}$, respectively. Here Ag(4f) peak at 268.3 eV were used for XPS calibration. Tentative assignment of the carbon binding energies reveals predominant C–C bond at 284.5 eV. Minor peaks at 282.5, 286, and 289 eV, attributable to C–Si, C–N, and C–O bonding structures, are also achieved. For N(1s) peak, the 397.5 and 399.8 eV binding energies are related to the N(1s)-Si and the N(1s)-C, respectively. The peaks centered at 102.9 and 100.3 eV are assigned to Si–N and Si–C bondings. Therefore, the covalent bonds among Si, C, and N in SiCN products are formed.

C. Raman characterization

Figure 4 shows the Raman spectrum obtained from the samples by the SiH$_4$ flux at 0, 8, and 20 sccm, respectively. Two strong peaks at about 1359 and 1600 cm^{-1} and several weak peaks at higher wave number can be clearly seen. The two strong peaks at 1359 and 1600 cm^{-1} are attributed to the D band and the G band, respectively. The D band is related to the amount of disordered or imperfect graphitic structure. The combination of D and G modes at 2943 cm^{-1} and 2D mode at 2730 cm^{-1} appear in the higher-order bands.

As shown in Fig. 4, the ratio of intensity of D band to G band (R) increases from 0.62 to 0.85 when SiH$_4$ flux reach to 20 sccm, that is to say, the higher Si concentration results in the higher defect density in SiCN nanotubes. The D bands in the Raman spectra of nanotubes originate from the finite particle size or lattice distortion, which is the main reason why the relative intensity of the D mode to the G mode increase while the Si concentration increasing.
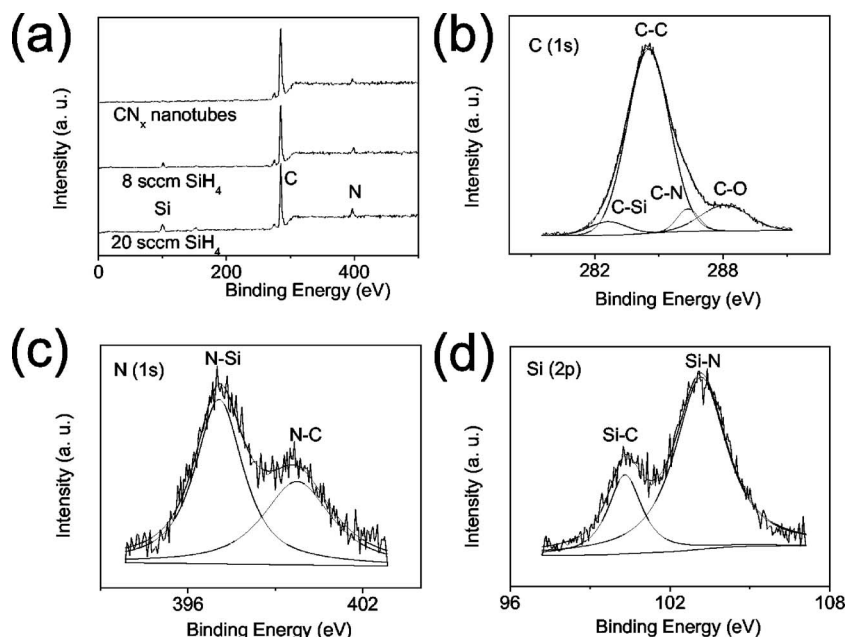
FIG. 3. (a) Broad XPS spectra of the three SiCN nanotube samples, grown at the SiH$_4$ flux of 0, 8, and 20 sccm, respectively; (b) XPS spectrum of C 1s; (c) XPS spectrum of N 1s; and (d) XPS spectrum of Si 2p. Spectra (b)–(d) correspond to the sample grown at SiH$_4$ flux of 20 sccm.

D. Field emission property

Figure 5(a) shows the field emission current–voltage ($I-V$) curves of the three samples by the SiH$_4$ flux at 0 sccm SiH$_4$, 8 and 20 sccm, respectively. The threshold field, defined as the field that causes an emission current of 1 μA/cm^2, varies from 4.2 to 6.8 V/μm. With the increasing Si concentration, the emission current decreases at the same applied voltage.

Furthermore, we studied the influence of ambient pressure on the field emission stability. Figure 5(b) shows the time-dependent field current at three stages: at 3×10^{-6} Pa and 8×10^{-4} Pa by air introduction and then at 3×10^{-6} Pa by pump. The time of each stage is 30 min. In the first 30 min, the three samples were set at nearly the same emission current. After air introduction to the pressure of 8×10^{-4} Pa, the current of the CN sample decreases quickly, while the current of the sample prepared by SiH$_4$ flux of 20 sccm decreases slowly. For the sample prepared by SiH$_4$ flux of 8 sccm, the current data are between the earlier two cases. It is found that, the air introduction results in the decrease of field emission current of the CN nanotubes to about 60% of its original value. In previous reports, the undesirable effect of absorbed O$_2$ on the field emission of a CNT has been studied

experimentally and theoretically.[26–28] The reactive etching/oxidation of the CNTs are believed as the reason of field emission deterioration. It is the similar case for CN nanotubes as studied here. After evacuating the chamber to the pressure of 3×10^{-6} Pa again, the emission currents basically keep unchanged.

It is noted that, with the increasing Si concentration in the SiCN nanotubes, the field emission becomes more stable. Our results suggest that the SiCN nanotubes have better oxidation resistance behavior than carbon/CN nanotubes. When the SiCN nanotubes emit electrons under high electric field

FIG. 5. (a) Field emission $I-V$ curves of the SiCN nanotube samples grown at the SiH$_4$ flux of 0, 8, and 20 sccm, respectively; (b) Time- and ambient pressure-dependent field emission of the SiCN nanotube samples.
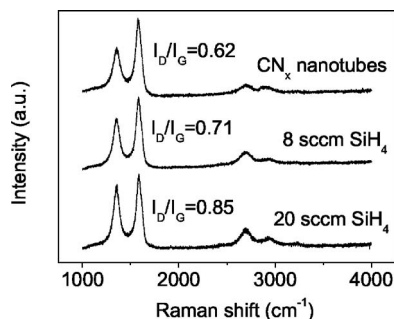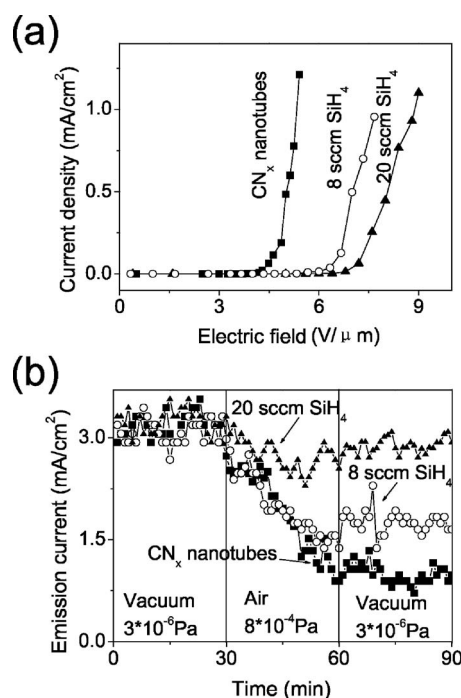

FIG. 4. Raman spectra of the SiCN nanotube samples with the three different compositions. The samples were grown at SiH$_4$ flux of 0 (a), 8 (b), and 20 sccm (c), respectively.

at low vacuum condition, the oxygen tends to bond with Si to form a thin SiO_x coating on the nanotube surface, so that the SiO_x layer effectively protects the SiCN nanotubes from further oxidation. But for carbon/CN nanotubes, the oxidation makes the nanotubes decayed, it will result in the deterioration of their field emission. Some researchers have already found that oxide coatings, such as SiO_2, on the CNTs can improve the field emission property and emission stability.[29] Recently, it was also reported that the thin SiO_x coated CNTs possess superior field emission behaviors and better lifetime characteristics.[30] In the present study, the structure of SiCN nanotubes has been characterized carefully by TEM after the field emission experiments. A thin SiO_x layer ($\sim 1-2$ nm) on nanotube surface is found, which acts as a protective layer. Therefore, SiCN nanotubes appear to be more stable as field emitter.

IV. CONCLUSION

In summary, MPCVD is an efficient method for growing large-scale aligned SiCN nanotube arrays. Various growth parameters have been used to control the microstructure and chemical composition of the nanotubes, as studied by HRTEM, EELS, XPS, and Raman spectroscopy. It is found that the field emission of SiCN nanotubes shows more favorable oxidation resistance characteristics, which suggests the SiCN nanotube is a stable semiconductor field emitter.

ACKNOWLEDGMENTS

[1] S. Hofmann, C. Ducati, B. Kleinsorge, and J. Pobertson, Appl. Phys. Lett. **83**, 4661 (2003).
[2] O. J. Lee and K. H. Lee, Appl. Phys. Lett. **82**, 3770 (2003).
[3] V. V. Zhirnov, E. I. Givarfizov, and P. S. Plekhanov, J. Vac. Sci. Technol. B **13**, 418 (1995).
[4] W. B. Choi, D. S. Chung, J. H. Kang, H. Y. Kim, Y. W. Jin, I. T. Tan, Y. H. Lee, J. E. Jung, N. S. Lee, G. S. Park, and J. M. Kim, Appl. Phys. Lett. **75**, 3129 (1999).
[5] N. de Jonge, Y. Lamy, K. Schoots, and T. H. Oosterkamp, Nature (London) **420**, 393 (2002).
[6] J. M. Bonard, J. P. Salvetat, T. Stockli, L. Forro, and A. Chatelain, Appl. Phys. A: Mater. Sci. Process. **69**, 245 (1999).
[7] W. A. de Heer, A. Chatelain, and D. Ugarte, Science **270**, 1179 (1995).
[8] M. J. Fransen, T. L. van Rooy, and P. Kruit, Appl. Surf. Sci. **146**, 312 (1999).
[9] J. M. Bonard, K. A. Dean, B. F. Coll, and C. Klinke, Phys. Rev. Lett. **89**, 197602 (2002).
[10] K. A. Dean and B. R. Chalamala, Appl. Phys. Lett. **75**, 3017 (1999).
[11] A. Wadhawan, R. E. Stallcup, and J. M. Perez, Appl. Phys. Lett. **78**, 108 (2001).
[12] W. K. Yi, T. W. Jeong, S. G. Yu, J. N. Heo, C. S. Lee, J. H. Lee, W. S. Kim, J. B. Yoo, and J. M. Kim, Adv. Mater. **14**, 1464 (2002).
[13] R. H. Reuss and B. R. Chalamala, Inf. Disp. **17**, 28 (2001).
[14] F. G. Tarntair, C. Y. Wen, L. C. Chen, J. J. Wu, K. H. Chen, P. F. Kuo, S. W. Chang, Y. F. Chen, W. K. Hong, and H. C. Cheng, Appl. Phys. Lett. **76**, 2630 (2000).
[15] N. M. Park, S. H. Kim, and G. Y. Sung, J. Appl. Phys. **94**, 2725 (2003).
[16] C. W. Chen, M. H. Lee, L. C. Chen, and K. H. Chen, Diamond Relat. Mater. **13**, 1158 (2004).
[17] C. W. Chen, C. C. Huang, Y. Y. Lin, L. C. Chen, K. H. Chen, and W. F. Su, Diamond Relat. Mater. **14**, 1010 (2005).
[18] L. C. Chen, K. H. Chen, S. L. Wei, P. D. Kichambare, J. J. Wu, T. R. Lu, and C. T. Kuo, Thin Solid Films **355–356**, 112 (1999).
[19] R. Riedel, H. J. Kleebe, H. Schonfelder, and F. Aldlnger, Nature (London) **374**, 526 (1995).
[20] K. H. Wu, E. G. Wang, J. Qing, and G. C. Xu, J. Appl. Phys. **83**, 1702 (1998).
[21] X. C. Ma, E. G. Wang, W. Zhou, D. A. Jefferson, J. Chen, S. Z. Deng, N. S. Xu, and J. Yuan, Appl. Phys. Lett. **75**, 3105 (1999).
[22] G. Y. Zhang, X. C. Ma, D. Y. Zhong, and E. G. Wang, J. Appl. Phys. **91**, 9324 (2002).
[23] D. Y. Zhong, S. Liu, G. Y. Zhang, and E. G. Wang, J. Appl. Phys. **89**, 5939 (2001).
[24] X. C. Ma and E. G. Wang, Appl. Phys. Lett. **78**, 978 (2001).
[25] J. Casanovas, J. M. Ricart, J. Rubio, F. Illas, and J. M. Jimenez-Mateos, J. Am. Chem. Soc. **118**, 8071 (1996).
[26] W. Q. Han, P. Kohler-Redlich, T. Seeger, F. Ernst, M. Ruhle, N. Grobert, W. Hsu, B. H. Chang, Y. Q. Zhu, H. W. Kroto, M. Terrones, and H. Terrones, Appl. Phys. Lett. **77**, 1807 (2000).
[27] Z. L. Wang, R. P. Gao, W. A. de Heer, and P. Poncharal, Appl. Phys. Lett. **80**, 856 (2002).
[28] W. S. Wang, L. M. Peng, J. Y. Wang, and Q. Chen, J. Phys. Chem. B **109**, 110 (2005).
[29] V. V. Zhirnov, W. B. Choi, and J. J. Hren, Appl. Surf. Sci. **94–95**, 123 (1996).
[30] J. S. Moon, P. S. Alegaonkar, J. H. Han, T. Y. Lee, J. B. Yoo, and J. M. Kim, J. Appl. Phys. **100**, 104303 (2006).